

# Fabrication of texturing tool to produce array of square holes for EDM by abrasive water jet machining

Vijay Kumar Pal<sup>1</sup> · S. K. Choudhury<sup>1</sup>

Received: 29 March 2015 / Accepted: 21 September 2015 / Published online: 12 October 2015  
© Springer-Verlag London 2015

**Abstract** In the present work, a novel abrasive water jet machining (AWJM)-based tool fabrication strategy has been proposed and implemented to make electrical discharge machining (EDM) tools for large-area texturing. The novelty of the work lies in the path strategy proposed for jet movement that moves along two raster paths placed at 90° to each other. By using this path strategy, micro-tools of EDM for machining arrays of square holes were fabricated by AWJ milling process. Based on selected parameters of AWJ process (step-over, traverse speed, path strategy), micro-tools were fabricated on brass and copper sheets. The quality of the kerf obtained during machining by AWJ is conventionally measured using the taper angle. It is explained here how this kind of measurements fall short of quantifying the quality of blind features generated in modern applications of AWJM. These generated features can be accurately measured using highly sensitive techniques of 3D optical profilometer. Based on these measurements, a model based on two performance indices, namely Area-Based Performance Index (API) and Curve-Based Performance Index (CPI) were introduced to analyse such fabricated tools. The technology of large-area texturing to make the overall process fast, by producing high-quality tools in less time, has been demonstrated by using the proposed methodology. Performance of such fabricated tools was investigated by performing experiments on EDM machine. Arrays of square blind holes (texture) were made on stainless steel and Ti-6Al-4V alloy sheet using Die sinking mode EDM. The

depth of texture was measured through 3D optical profilometer and was found to be in the range of 10 to 100 μm. The dimensions of textured features were found deviating from the tool dimension due to taper present on side-walls of micro-tools produced through AWJM.

**Keywords** AWJM · Path strategy · API · CPI · Texturing · EDM · Electrode (tool)

## 1 Introduction

Electrical discharge machining (EDM) is a nonconventional material removal process to provide shape on any electrical conductive material irrespective of its hardness. It is mostly used in precision manufacturing industry to manufacture complex 3D components of macro- to nanoscale sizes with acceptable dimensional accuracy [1]. In EDM process, the high thermal energy of an electric spark is used to remove the excess material from the workpiece and the mirror image of the tool (electrode) shape is obtained on the workpiece surface. The tool electrode is an essential component for the process, and the EDM performance is strongly dependent on the electrode material, shape, design, and manufacturing [2]. But micro-tool design for EDM is a big challenge in this process. The appropriate method to fabricate electrode (tool) is still a big challenge in manufacturing industries. Various methods were used to fabricate tools for EDM. However, each method has its advantages and disadvantages with respect to machining performance and costs. Materials with properties of high electrical conductivity and high-melting point like brass, copper (Cu), graphite, and Cu–tungsten are usually used in EDM [3]. From the literature review, it is clear that the fabrication for EDM electrode is a major time-consuming and cost-carrying factor. The increment in the demand of micro-

✉ Vijay Kumar Pal  
vijayp@iitk.ac.in

S. K. Choudhury  
choudhry@iitk.ac.in

<sup>1</sup> Department of Mechanical Engineering, Indian Institute of Technology Kanpur, Kanpur, India

feature and its complex design pushed EDM electrode manufacturing by traditional methods, which takes more time and cost, as very less sources/companies are available to fabricate them [4].

Abrasive water jet machining (AWJM) is a state-of-the-art non-traditional machining process making use of high-pressure water converted to high-velocity jet mixed with abrasives with an ability to cut various materials ranging from soft material like plastics, rubber, wood, etc., to hard materials like titanium and inconel. Originally, AWJM technique was only used for linear cutting and shape cutting of difficult-to-cut materials [5].

Nowa's researchers have also started experimenting on generating blind features using AWJM. For generating blind features like pockets and channels, several authors used the multiple passes linear traverse cutting as milling strategy. This principle is based on the superposition of several passes to obtain a cavity of defined geometry. The lateral distance between the single kerf and passes is the main parameter in this process [6], which is kept less than the diameter of the jet ( $d$ ). Hashish [7] used the principles of rotary table and masking to perform a controlled depth milling of iso-grid structures. Fowler et al. have developed the process of controlled depth milling (CDM) and studied the effects of various parameters like traverse speed, jet impingement angle, milling direction, grit size, etc. [7] on surface characteristics while machining titanium alloy. While investigating the role of machinability in AWJ-CDM for materials like AL 6061 alloy, AL 2024, brass 353, titanium AISI 304 (SS), and tool steel, the authors observed that time taken to mill increases as the depth of milling increases non-linearly due to loss of energy of jet and increase in standoff distance (SOD) [8]. The literature survey reveals that the geometrical features, like channels (single slot) and pockets (closed loop path), can be fabricated using AWJ milling. Pal and Chaudhury in 2014 introduce a novel path strategy to fabricate some more complex 3D features [9]. They developed a concept to fabricate micro-pillars of different aspect ratios, and these features were fabricated by keeping the step-over (SO) more than the diameter of jet ( $1.25d$ ) such that there was no superimposition of the parallel passes of the jet. In the present study, a novel path strategy is introduced to fabricate the micro-tool of different shapes (here, array of square spikes) using the concept of multi-pass linear traverse cutting. Here, the distance between the two parallel passes was also kept more than the nozzle diameter [10].

The objective of this research is to develop a concept for producing micro-tools by AWJ milling process, which would be further utilized as texturing tools for EDM process. For the rapid generation of textured surfaces. The viability of the process of producing textured surfaces having micro-features on larger area is to be experimentally investigated. Tools to produce large area texturing (arrays of square holes) on hard materials were fabricated on brass and copper sheets by

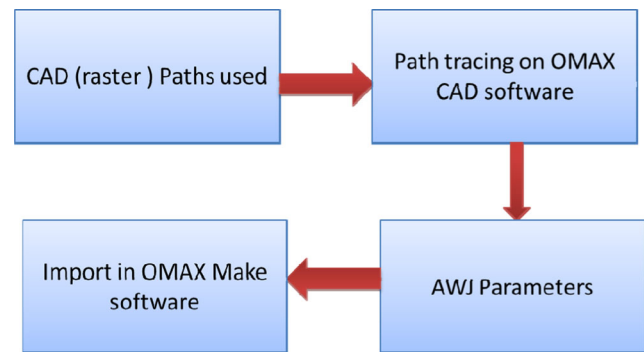


**Fig. 1** Tool path generation on controller (OMAX)

AWJ process. Primary experiments were carried out to determine suitable range of process parameters, based on which, tools were fabricated. EDM is one of the advantageous methods to provide shape on very hard material. The performance of such fabricated tools by AWJ milling process was shown by performing experiments on EDM machine to make texture on stainless steel and Ti-6Al-4V sheet.

## 2 Concept to produce micro-tool for texturing

### 2.1 Process flow of the proposed methodology

The process flow to fabricate texturing tool by AWJ process in the present work is as follows:

**Geometry creation** First step of the process is to generate CAD geometry of the required shape and import into the controller of the machine (OMAX Layout). The path strategy involved creation of two different paths in Autodesk Inventor that are superimposed on each other in subsequent jet passes in such a way that the resultant of the two is a channel consisting of square pillars (detail explanation is given in Section 2.3)

**Path tracing** Figure 1 shows the steps used in path tracing. After importing the “.dxf” file of the jet path in the OMAX CAD software, path tracing was done and the starting point of the cut was specified after selecting the machining parameters.

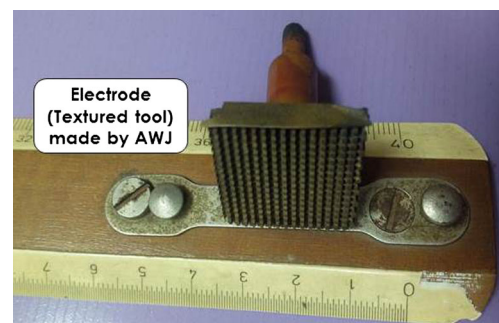
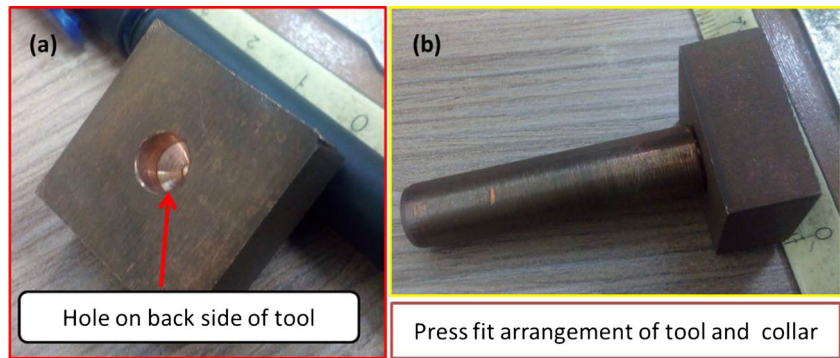


**Fig. 2** Textured tool fitted in collar by brazing process

**Fig. 3** **a** Hole on copper tool to insert the collar. **b** Collar inserted into produced copper tool by AWJ milling textured tool fitted in collar



The nozzle of the machine moves along the tool path used in the methodology.

**Parameters specification** Selected process variables (pressure, standoff distance, and step-over) were used as input parameters for the machine to achieve required depth and geometry of the feature.

**Fitting the collar for EDM** Once the texture tool was fabricated, it was fitted to the collar as tool shank for using it on EDM (Fig. 2). Tools were fabricated on brass and copper sheet of 12 mm thickness, and collar was fitted into the tool. Figure 3a shows the hole on back side of the tool, and Fig. 3b shows the collar fitted into it by press fit arrangement.

**2.2 Experimentation**

Experiments were carried out using an abrasive water jet machining centre (model no. 5226, M/s OMAX, USA make). Table 1 shows the specifications of the machine. In AWJM process, highly pressurized water is mixed with abrasive particles in a mixing tube (Fig. 4). The abrasive water jet is focused through a focusing tube before making an impact on the selected area on the work material. In this work, brass and copper sheets were used as work material for fabrication of tools. Test samples were ground before subjecting to AWJM in order to improve the flatness of the resulting tool. Figure 5 shows the surface roughness profile of workpiece.

**Table 1** Machine specification

|                          |              |
|--------------------------|--------------|
| Maximum traverse speed   | 4572 mm/min  |
| Jet impingement angle    | 90°          |
| Orifice diameter         | 0.33 mm      |
| Abrasive flow rate       | 0.226 kg/min |
| Mixing tube diameter     | 0.762 mm     |
| Mixing tube length       | 101.6 mm     |
| Maximum working pressure | 45 kpsi      |

**2.3 Path strategy used to fabricate tool (array of square pattern)**

The earlier works of Fowler et al. in AWJM [11, 12] report a new AWJM methodology called controlled depth milling (CDM) to create blind pockets on metal surface by intentionally overlapping the consecutive AWJM passes to produce cavities of depth less than the work-piece thickness. The similar strategy has been followed in the present work to fabricate array of features but without overlapping of the cavities/paths.

For this purpose, a novel path strategy is introduced to fabricate micro-texturing tool by AWJM process. The resulting machined surface is to be used as a tool in the EDM process. The path strategy has been extended from the work of Pal and Chaudhury [9] and briefly explained with the help of Fig. 6a. Here, machining was carried out by keeping the distance between two successive passes

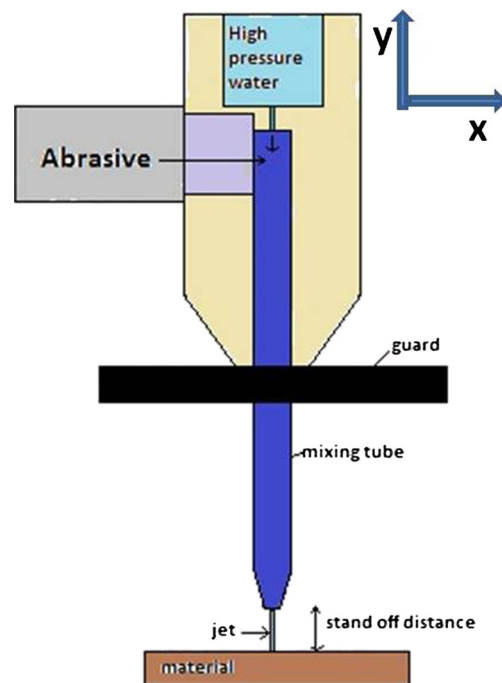


**Fig. 4** AWJM process (nozzle and mixing chamber)

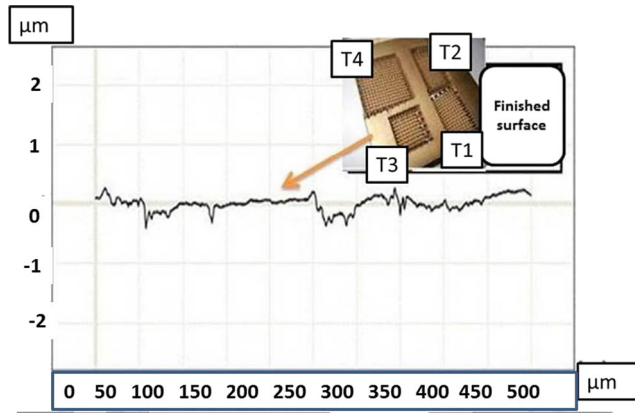


Fig. 5 Surface roughness profile of grinded brass sheet

(also known as step-over (SO)) more than the diameter of jet such that there was no superimposition of the parallel passes of the jet. By this manner, some material in the form of strip was retained between two consecutive passes during machining, as shown in the first and second raster paths (Fig. 6a). Both the raster paths cross each other perpendicularly.

It can be clearly seen that the two crossed raster paths generate the arrays of square on the same area. The cross motions of nozzle along these raster paths leave some material in between their consecutive passes which results in the square pillars. The real image of one of the fabricated tool (T3) is shown in Fig. 6b.

Based on the present strategy, four different tools on brass sheet and two tools on copper sheet were fabricated with different geometric configurations by varying process parameters associated with the AWJM. The quantitative features of these tools are listed in Table 2, and the tools are shown in Fig. 7. If the step-over distance is changed, the number of the resulting features (spikes) changes. Similarly by varying the traverse speed, the depth of cut (hence, height of the spikes) can be varied.

Fig. 6 a Path strategy to fabricate tool of array of square pins. b Real image of fabricated tool (T3)

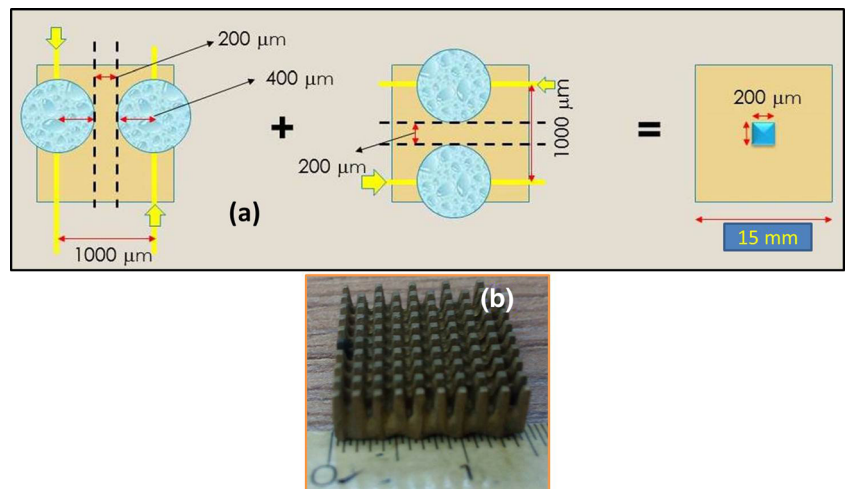


Table 2 Parameters considered for AWJM

|                         | Brass          |                |                |                | Copper         |                |
|-------------------------|----------------|----------------|----------------|----------------|----------------|----------------|
|                         | T <sub>1</sub> | T <sub>2</sub> | T <sub>3</sub> | T <sub>4</sub> | T <sub>5</sub> | T <sub>6</sub> |
| Step-over (mm)          | 1.1            | 1.3            | 1.3            | 1.5            | 1.1            | 1.3            |
| Traverse speed (mm/min) | 3500           | 3500           | 2500           | 2500           | 3500           | 3500           |
| Area (mm <sup>2</sup> ) | 15×25          | 15×25          | 15×25          | 25×25          | 25×25          | 25×25          |

### 3 Analysis of the fabricated tools

Abrasive water jet machining (AWJM) is a well-known process for machining any material irrespective of their hardness. Most of the works done using AWJM is through cutting, but of late, researchers have also started experimenting on generating blind cut features by AWJ milling process. Kerf taper is an undesirable geometrical feature inherent to AWJ which restricts the process from many commercial purposes and also difficult to measure accurately. Quality of the kerf is conventionally measured using the taper angle (Fig. 8). Taper angle is expressed as (Eq. 1) follows:

$$\tan\theta = \frac{W_b - W_t}{2 \times H} \tag{1}$$

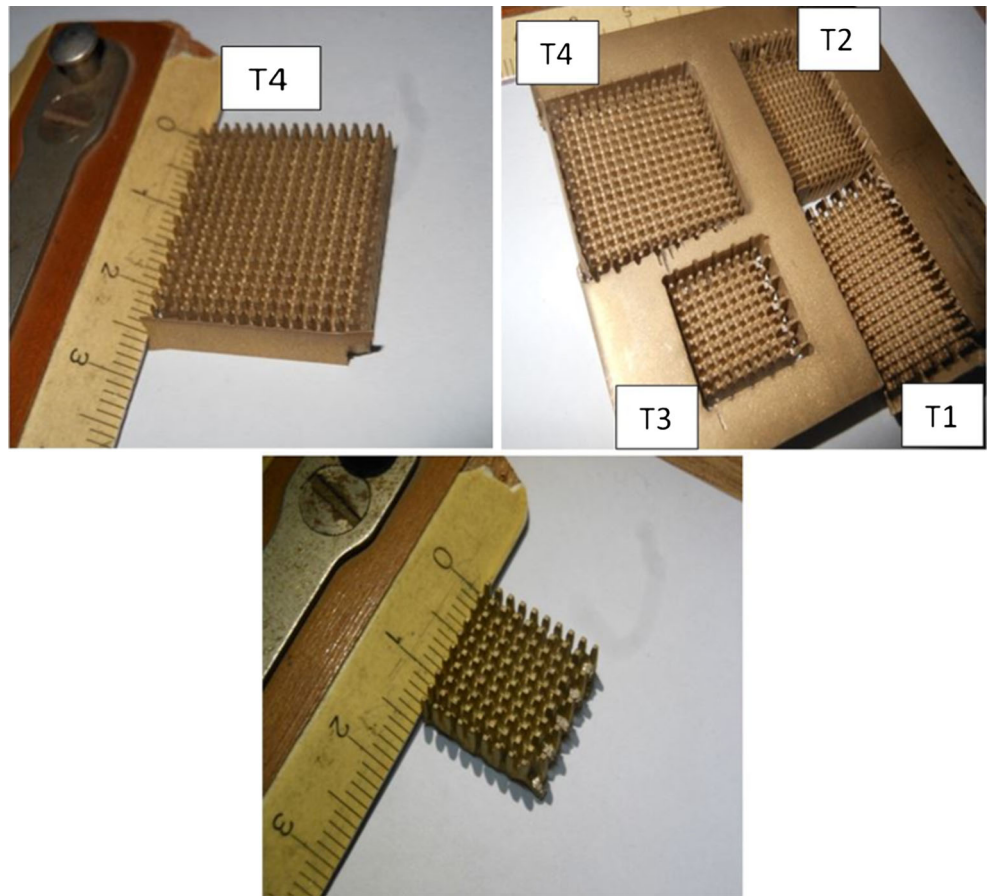
where  $\theta$ =taper angle

- $W_b$  bottom width
- $W_t$  top width
- $H$  thickness of the material

But the method explained above falls short of quantifying the quality (sidewall profile) of blind features generated in modern application of AWJM. For example, consider Fig. 9, with four different machined surfaces with the same taper angle. One can conclude from this illustration that even though the taper angles are the same, the quality of machining varies significantly across these four cuts. Depending upon the



**Fig. 7** Fabricated tools by AWJM on brass sheet



desired surface, one of these cuts will be the best outcome. Thus, the taper angle measure performs poorly when it comes to accurately quantify the machining quality for small features.

To explain the proposed technique, consider the following machining operation where the aim is to carve parallel channels of rectangular cross section of micron dimensions (Fig. 10), i.e., vertical walls like “abf” and “ecd.”

Since workpiece material will resist fracture by impinging jet and kinetic energy of the jet also losses its energy while

going along the depth, one cannot create ideal features and practical implementation will inevitably contain some imperfections. Dotted lines (Fig. 10) show the imperfections in the shape (kerf profile).

Kerf generation during AWJM is shown in Fig. 10; the machining process will leave more material than desired. An alternate way to define machining quality can be based on the comparison of cross-sectional areas of the machined cuts, i.e.,  $A_{\text{practical}} - A_{\text{ideal}}$ , quantifying the machining quality. In order to compare machining quality across various process

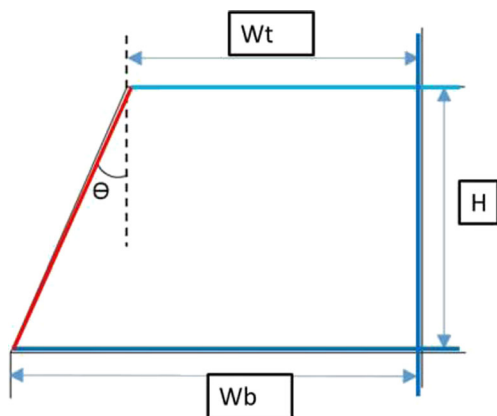


**Fig. 8** Taper angle calculation

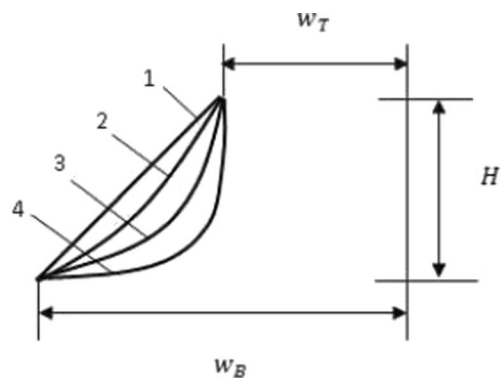


**Fig. 9** Taper angle between two points will same but profiles may varies

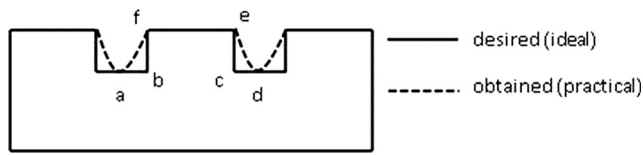


Fig. 10 Ideal and practical blind cut of AWJ process

parameters, this is modified to give a normalized Area-Based Performance Index (API) as follows (Eq. 2):

$$API = A_{ideal} / A_{practical} \tag{2}$$

Here,  $A_{ideal}$  is the cross-sectional area of the desired surface, while  $A_{practical}$  is the area obtained in machining. For the job considered here (Fig. 10), area “bcefb” is the desired profile, while “abcdefa” is the machined profile. As API approaches unity, machining quality improves with unity being the ideal profile.

This Area-Based Performance Index better represents the machining quality compared to the taper angle-based quality definition. For more accurate representation, however, we propose a Curve-Based Performance Index (CPI) which utilizes the curve length of the machined surface. CPI is expressed in Eq. 3 as the following:

$$CPI = s_{ideal} / s_{practical} \tag{3}$$

Here,  $s$  denotes the arc length of the desired surface. In the case considered here,  $s_{ideal}$  is the height of the hill (or depth of cut) and  $s_{practical}$  is the arc length of the actual machined surface (Fig. 11). Similar to API, as CPI approaches unity, the quality of machined surface increases. The accuracy of these calculated values will greatly depend on the accuracy of measurement of the machined surface which is possible only through detailed experimentation like optical profilometer measurements. Though such experiments, an experimental curve shape obtained is symbolically represented as  $y=f(x)$ . The equation of the kerf profile could be obtained by using the methodology given by Pal and Choudhary. Data obtained by profilometer can be used directly to

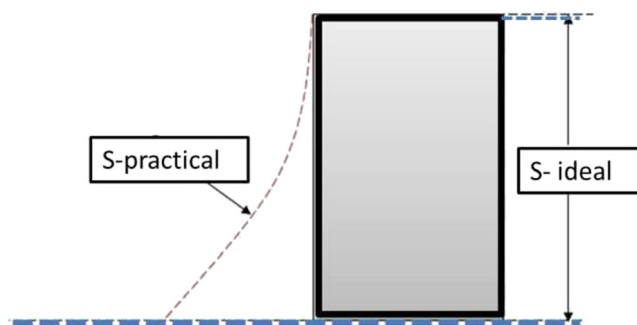


Fig. 11 Arc length for an ideal and practical condition

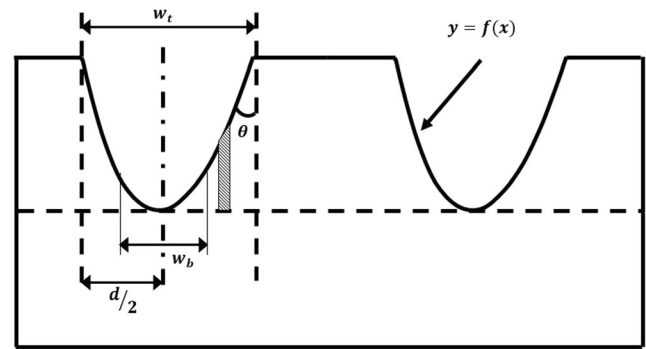


Fig. 12 Calculation of API and CPI

numerically calculate area and arc length from numerical integration of the following analytical formulae:

Figure 12 shows two identical passes of AWJ used to machine and traverse along the same direction. Material of width (b) left between two passes more than the diameter (d) of jet.

Now, area under of kerf profile ODAO is given by Eq. 4:

$$Area = \int_0^{d/2} y \cdot dx \tag{4}$$

$$API = A_{ideal} / A_{practical}$$

API of given geometry is expressed by Eq. 5:

$$API = \frac{A_{ideal}}{A_{ideal} + 2 \int_0^{d/2} y \cdot dx} \tag{5}$$

And the curve based performance index:  $CPI = s_{ideal} / s_{practical}$

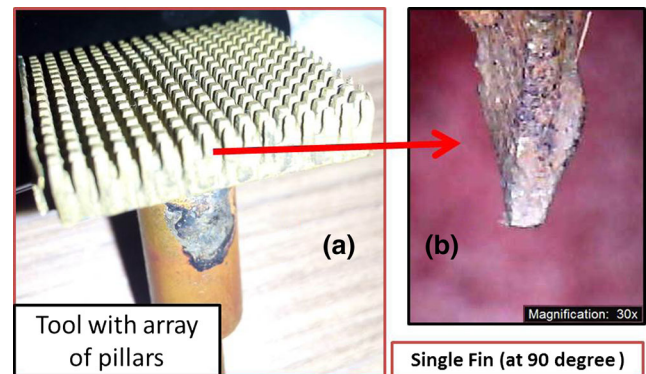


Fig. 13 Image of a arrays of fins of tool (T4) and b single fin

where the arc length (Fig. 11) can be calculated as (Eq. 6):

$$\text{Arc length}(s) = \int_0^{d/2} \sqrt{1 + \left(\frac{dy}{dx}\right)^2} \cdot dx \quad (6)$$

These parameters are defined such that they are valid for any two-dimensional feature (e.g., channel) machined through AWJM process.

Now, considering all the passes used in the identical present methodology, the abovementioned strategy could be used for analysis of the fabricated tools.

For a real machined surface, both the performance index values are less than one. Thus, the closer are the values of API and CPI to unity, the more ideal is the machined surface. Figure 13 shows the enlarge image of fins and tool (T4) obtained at various machining conditions.

Based on the state-of-art fabrication of 3D complex features using AWJ milling, the process is characterized by three main input parameters:

1. Step-over distance (SO): distance between two parallel consecutive machining passes, specified in terms of diameter of abrasive water jet, “d.”
2. Traverse speed (TS): the speed of motion of nozzle along the path traversed by the nozzle.
3. Pressure (P): is the operating pressure of the AWJ machine, which in turn dictates the depth of metal removal.

The step-over specifies the nature of material removal, i.e., overlapping passes will have SO less than “d” and non-overlapping passes will have SO greater than “d.”

In cutting paths used in the AWJ milling with variable traverse speed, the depth reached at each position depends upon the exposure time of jet on the workpiece surface. The kerf profile was not uniform along the passes of jet because the direction of jet changes, and consequently, the acceleration and deceleration occurs during machining. In this research work, traverse speed was assumed to be uniform to analyse the performance of parameters on shape of the fabricated tools.

From the present analysis, it was observed that, with the increase in step-over (SO), the values of performance indices API and CPI were found close to unity. This can be explained as follows: with a small SO distance (say, 1 mm), very less amount of backing material was available to support the mechanical forces exerted during the next pass, and hence, the surface produced was wavy in nature along with reduced dimensional quality. The features produced on brass tool (T4) of dimension  $600 \times 600 \mu\text{m}$  (Fig. 13) was found to be of reasonably good quality as its API was found very close to one to a better material removal mechanism (brittle fracture). The

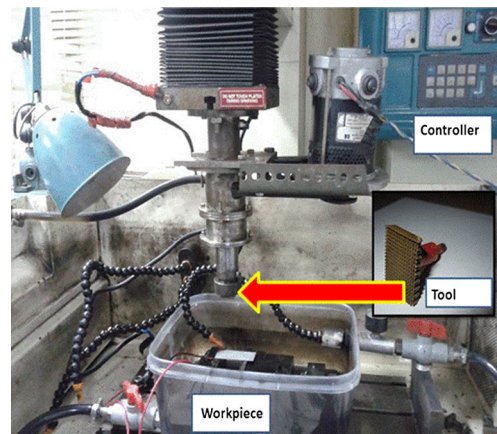


**Fig. 14** EDM set up for texturing

values of API and CPI were also found to be closer to unity on tool of brass material as compared to copper.

#### 4 Performance of textured tool in electric discharge machining

In this section, experiments were conducted on an electrical discharge machining (EDM) using the brass and copper tools, generated by AWJM, as electrodes to investigate their performances. The technology of proposed concept (texturing tool fabrication) has been demonstrated by keeping in mind of the rapid generation of the texturing tool to produce micro-texturing on large area. The tools produced by AWJM of various sizes were used as tool (electrode) in the EDM. A shank in the form of a copper cylinder was brazed to these pieces to use them as EDM tool.

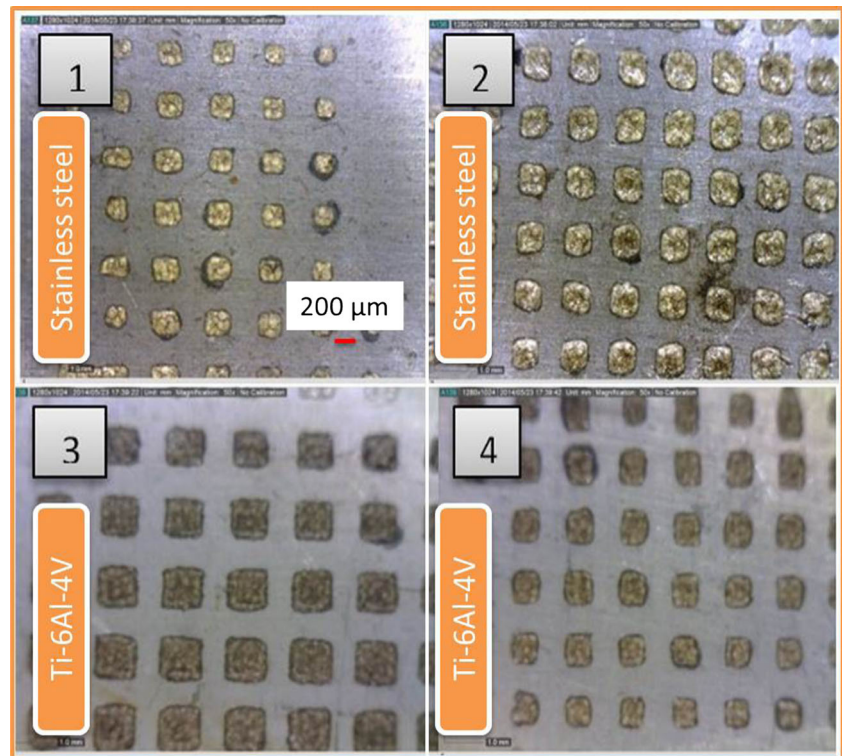
The experimental arrangement is pictorially shown in Fig. 14. The performance of tools thus fabricated was investigated in an EDM setup. The process parameters for this machining were selected based on micro-features machining and presented in Table 3. The experiments were conducted on Ti-6Al-4V alloy and stainless steel sheets of 1 mm thickness. This work aims to achieve large area texturing of arrays of blind square holes on sheets. All the four tools of brass material developed in the AWJM were used in EDM to machine these materials. The responses of texturing tools were characterized by the depth and geometry of the texture obtained on these sheets. The images of the surfaces machined using the

**Table 3** EDM parameters for brass and copper tools

| Sample no. | Parameter     | Brass             | Copper            |
|------------|---------------|-------------------|-------------------|
| 1          | Current       | 5 A               | 3 A               |
| 2          | Voltage       | 75 V              | 75 V              |
| 3          | Pulse on time | 150 $\mu\text{s}$ | 150 $\mu\text{s}$ |
| 4          | Duty factor   | 72 %              | 72 %              |



**Fig. 15** Textured images by various brass tools (T1, T2, T3, and T4)



four tools enlisted in Table 2 are shown in Fig. 15. The numbering is in accordance with the tool numbers in Table 2. For the first two images (Fig. 15), the workpiece is stainless steel, while for the latter two, titanium alloy workpiece was used. Tool 1 (T1) had a smaller step-over distance than tool 2 (T2). This resulted in smaller fins on the tool and subsequently the features produced during EDM. This is apparent from Fig. 15. Similarly, tool 3 had smaller step-over than tool 4, thus producing smaller features on the corresponding workpiece. It can also be observed from these figures that the shapes produced on these sheets correspond to the texturing on the tool.

Enlarged image of one of the surfaces machined (corresponding to tool 4) is shown in the Fig. 16. The measurement shows that the produced features are of an approximate dimension of  $700 \times 700 \mu\text{m}$ . The image of the corresponding tool is shown in Fig. 7. The area of the top surface of each square fin is  $600 \times 600 \mu\text{m}$ , and the enlarged image of the texture (replica) produced by these tools are shown in Fig. 18. This discrepancy between the tool dimension and workpiece can be explained as follows: as the tool produced by AWJM has taper along the height of the fins. During EDM, the tool also undergoes some wear. Because of these, the tool

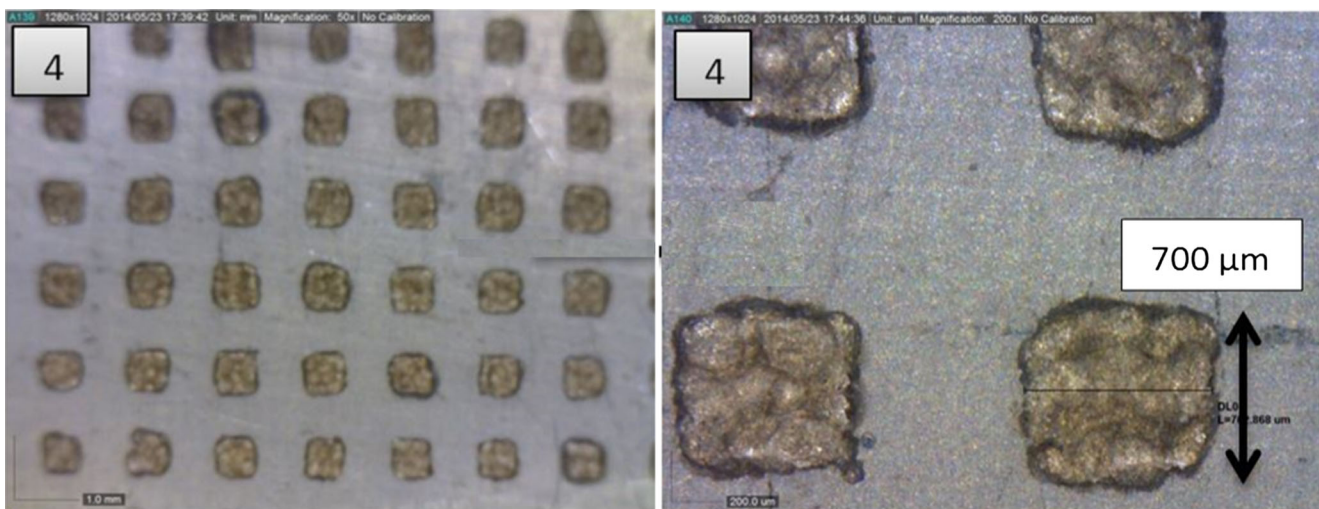
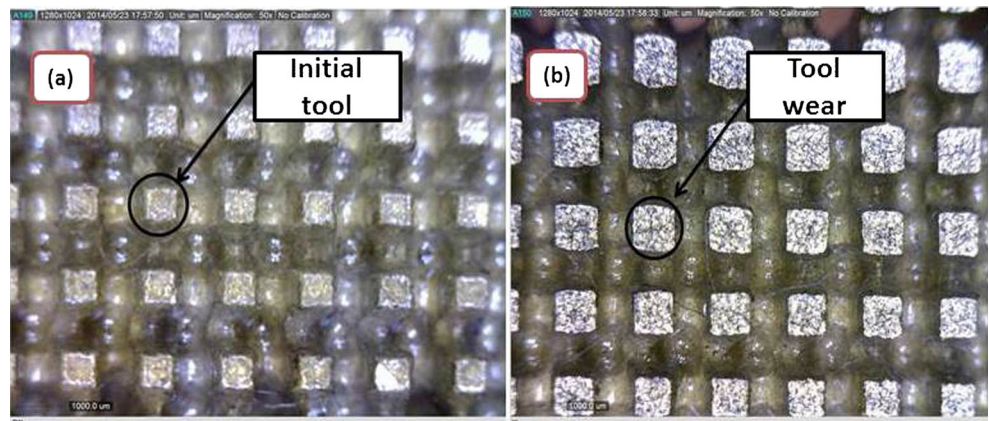


**Fig. 16** Enlarge view of texture obtained by tool (T4)



**Fig. 17** Images of (a) new and (b) wear tool



area responsible for EDM machining increases in time and produces features larger than the initial tool dimensions. However, due to EDM, die sinking mode workpiece (array of square holes) got machined sidewise also as the tool used was not masked from the sides [13]. This image of the tool wear is shown in Fig. 17. Figure 17a shows a new tool, and Fig. 17b shows the corresponding worn out tool. Because of this taperness in the tool, the resulting feature is also expected to be tapered along the depth direction. This is confirmed by the optical image of the machined workpiece surface as shown in Figs. 18 and 19. The depth of texture was measured through 3D optical profilometer of FOV (2×) and objective (5×) embedded with vision 64 software.

The optical image of small texture (400×400 μm) is shown in Fig. 20.

Since titanium alloy is difficult to machine compared to stainless steel surface, therefore corresponding depth obtained after machining (texturing) was found less on titanium. This fact is also reflected by larger tool wear while machining the

titanium alloy surface. These comparisons can be justified since the same machining parameters were used while working on all these surfaces and tools.

Based on these arguments, the following trends are expected:

- Tool wear should be more while machining titanium surface (compared to stainless steel surface).
- Because of larger tool wear, the ratio of obtained textured profile area to the tool surface area should be larger on titanium.
- Depth of features should be less on titanium.
- For same operating parameters and machined surfaces, fractional wear should decrease with tool cross section.

Quantitatively, machining of stainless steel using tool cross sections 200×200 and 400×400 μm gives the features of dimensions 290×290 and 480×480 μm, respectively. Similarly, tools of dimensions 400×400 and 600×600 μm produced features of cross sections 450×450 and 700×700 μm, respectively, while machining titanium surface. Depth of cut on titanium was found in the range of 10–30 μm which was quite less than stainless steel machining (50–70 μm). This is because the stainless steel is easier to machine than titanium alloy.

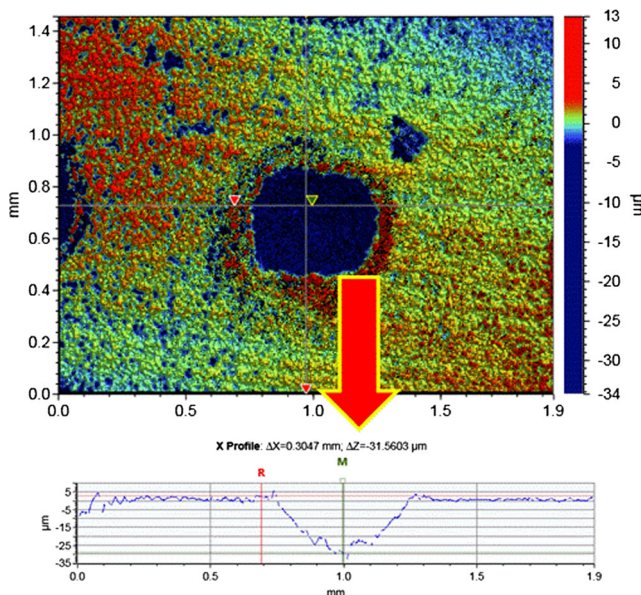


**Fig. 18** Optical image (3D) of the square hole texture

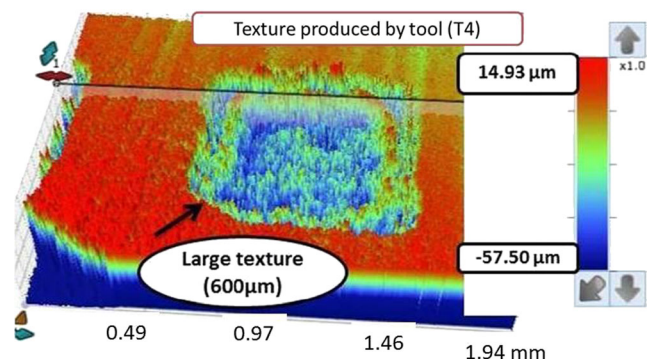


**Fig. 19** Optical image (3D) of large textured produced by tool (T4)

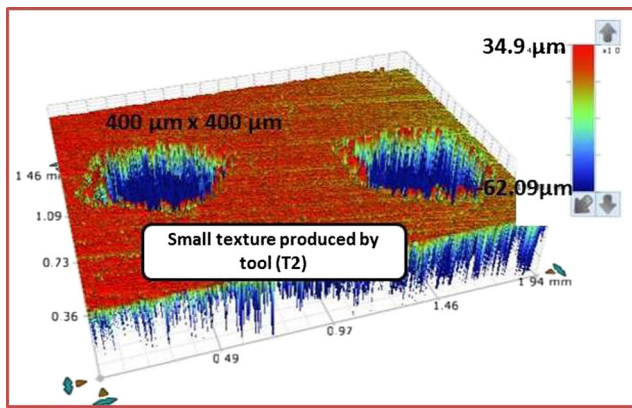


**Fig. 20** Optical image (3D) of texture (*square blind hole*) produced by EDM

Initially brass was chosen as tool material for generating micro-texture using EDM process, as brass shows better characteristics for mechanical erosion through AWJM than commonly used copper which is necessary to fabricate sound micro-features, i.e., an array of square micro-pockets in the present case. But as the features of the brass tools fabricated by AWJ milling were very fine and high heat generated during EDM could lead to damages of the geometry of tool features, so more commonly used copper was selected as another tool material. Copper, due to its high conductivity, is known to give better results as far as the tool wear in EDM is concerned. Input parameters are given in Table 3. Images of achieved large area texturing produced by these tools on stainless steel sheet are shown in Fig. 21.

## 5 Conclusion

It is concluded that the capability of AWJM process can be extended to fabricate micro-tool (electrode) for EDM. Present work shows the path strategy to fabricate tool (arrays of square pin) on brass and copper sheet. Performance of tools were analysed by conducting experiments on stainless steel and

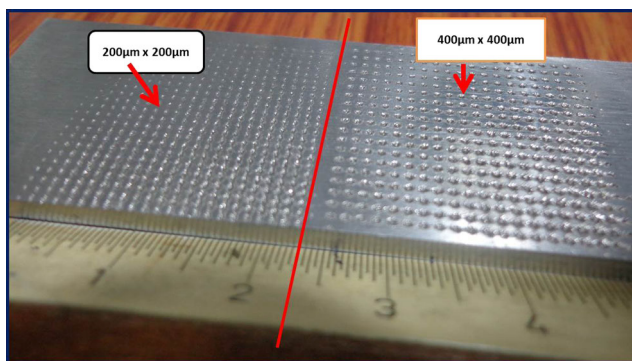


**Fig. 21** Large area texturing (*arrays of square holes*) produced by copper tools on stainless steel sheet

Ti-6Al-4V sheet. Based on the observations of present investigation, the following conclusions can be drawn:

- As the operating step-over increases, the performance of AWJ milling process improves because jet impinges on the area of sufficient backing material and which is able to bear the mechanical forces exerted during the next pass of high-pressurized jet. (Since API and CPI tend to unite).
- Smaller step-over produces the smaller fin (top area), e.g., tool 1 (T1) has a smaller step-over distance than tool 2 (T2). This results in smaller fins on the tool and subsequently the features produced during EDM.
- The deviation in dimensions of feature produced on the workpiece (textured surface) from the dimensions of micro-tool produced by AWJM may be attributed to two factors: first, due to the taper present on the tool which is due to inherent characteristics of the AWJM jet that produces kerf along the fin length and another reason might be that during EDM process, the sidewalls of the micro-features (blind square cavities) also get machined due to EDM being used in die sinking mode and the tool features used are not masked on the sides.

## References

1. Rajurkar KP, Sundaram MM, Malshe AP (2013) Review of electrochemical and electro discharge machining. *Procedia CIRP* 6:13–26
2. Fleischer J, Masuzawa T, Schmidt J, Knoll M (2004) New applications for micro-EDM. *J Mater Proc Technol* 149:246–249
3. Li L, Wong YS, Fuh JYH, Lu L (2001) Effect of TiC in copper-tungsten electrodes on EDM performance. *J Mater Proc Technol* 113:563–567
4. Zaw HM, Fuh JYH, Nee AYC, Lu L (1999) Formation of a new EDM electrode material using sintering techniques. *J Mater Proc Technol* 89–90:182–186
5. Kovacevic R (1991) Surface texture in abrasive water jet cutting. *J Manuf Syst* 10(1):32–40
6. Laurinat A, Louis H, Meier-Wiechert G (1993) A model for milling with abrasive water jet. In: Hashish M (ed) *Proceedings of the 7th American water jet, vol Proceedings of the 7th American Water Jet. Water jet Association, St. Luis*, pp 119–139
7. Hashish M (1994) Controlled-depth milling techniques using abrasive-waterjets. In: Allen NG (ed) *Jet cutting technology. Mechanical Engineering Publication Ltd, London*, pp 449–461
8. Pal VK, Tandon P (2011) Identification of role of machinability and milling depth on machining time in controlled depth milling using abrasive water jet. *Int J Adv Manuf Technol* 66:877–881
9. Pal VK, Choudhury SK (2014) Fabrication and analysis of micro pillars by using abrasive water jet machining. *J Proc Mater Sci* (6) 61–71
10. Pal VK, Choudhury SK (2014) Application of Abrasive water jet machining in fabricating micro tools for EDM for producing array of square holes, AIMTDR-2014, IIT Guwahati, India, 12–14
11. Fowler G, Shipway PH, Pashby IR (2005) Characteristics of the surface of a titanium alloy following milling with abrasive waterjets. *Wear* 258:123–132

12. Fowler G, Shipway PH, Pashby IR (2005) A technical note on grit embedment following abrasive water jet milling of titanium alloy. *J Mat Proc Technol* 159:356–368
13. Jain VK (2002) *Advanced machining processes electrochemical machining (ECM)*. Allied publishers, New Dehli, pp 232–279